

- Koenig, M., and Grabe, N. (2004). Highly specific prediction of phosphorylation sites in proteins. *Bioinformatics* **20**, 3620–3627.
- Laemmli, U. K. (1970). Cleavage of structural proteins during the assembly of the head of bacteriophage T4. *Nature* **227**, 680–685.
- Munafò, D. B., and Colombo, M. I. (2002). Induction of autophagy causes dramatic changes in the subcellular distribution of GFP-Rab24. *Traffic* **3**, 472–482.
- Olkkonen, V. M., Dupree, P., Killisch, I., Lutcke, A., Zerial, M., and Simons, K. (1993). Molecular cloning and subcellular localization of three GTP-binding proteins of the rab subfamily. *J. Cell Sci.* **106**, 249–261.
- Ostermeier, C., and Brunger, A. T. (1999). Structural basis of Rab effector specificity: Crystal structure of the small G protein Rab3A complexed with the effector domain of rabphilin-3A. *Cell* **96**, 363–374.
- Overmeyer, J. H., Wilson, A. L., Erdman, R. A., and Maltese, W. A. (1998). The putative “switch 2” domain of the Ras-related GTPase, Rab1B, plays an essential role in the interaction with Rab escort protein. *Mol. Biol. Cell* **9**, 223–235.
- Wittmann, J. G., and Rudolph, M. G. (2004). Crystal structure of Rab9 complexed to GDP reveals a dimer with an active conformation of switch II. *FEBS Lett.* **568**, 23–29.
- Yang, C., Mollat, P., Chaffotte, A., McCaffrey, M., Cabanie, L., and Goud, B. (1993). Comparison of the biochemical properties of unprocessed and processed forms of the small GTP-binding protein, rab6p. *Eur. J. Biochem.* **217**, 1027–1037.
- Zhou, F. F., Xue, Y., Chen, G. L., and Yao, X. (2004). GPS: A novel group-based phosphorylation predicting and scoring method. *Biochem. Biophys. Res. Commun.* **325**, 1443–1448.
- Zhu, G., Liu, J., Terzyan, S., Zhai, P., Li, G., and Zhang, X. C. (2003). High resolution crystal structures of human Rab5a and five mutants with substitutions in the catalytically important phosphate-binding loop. *J. Biol. Chem.* **278**, 2452–2460.

## [17] Assay of Rab25 Function in Ovarian and Breast Cancers

By KWAI WA CHENG, YILING LU, and GORDON B. MILLS

### Abstract

There is a multitude of critical steps during the pathogenesis of cancer that allow cells to acquire the ability to escape from normal controls on cell growth, to avoid programmed cell death, and to become malignant. Here, we describe a molecular approach that can be broadly applied to identify drivers of genomic aberrations in cancer development. In the process, areas of genomic aberrations and genes that are dysregulated by genomic amplification are identified by array comparative genomic hybridization (CGH) and transcription profiling, respectively, with major emphasis on coordinating amplification at the CGH and RNA level and on correlation with patient's outcomes. Once candidate genes are identified, we perform

functional genomics by manipulating levels in normal and tumor cells using RNAi or transfection, and assessing a battery of cellular functions including proliferation, anti-apoptosis, loss of contact inhibition, changes in cell signaling or transcriptional profiles, anchorage-independent growth, and *in vivo* tumor growth. We have successfully used this approach to identify the *RAB25* gene that has been implicated in the progression and aggressiveness of ovarian and breast cancers.

## Introduction

Cancer is a disease of genes resulting from genetic and epigenetic changes that occur within a single cell, allowing the cell to acquire an ability to bypass the cell cycle check point, to become resistant to growth inhibitory pathways, to bypass senescence and crisis, and to become immortal (Cavenee and White, 1999; Hanahan and Weinberg, 2000). Many of the genes responsible for the development of malignancy fall into the class of oncogenes (Weinberg, 1996). The normal structure of a resident proto-oncogene may be converted to a dominant oncogene by mutations or chromosomal rearrangements. Occasionally, the protooncogene is not mutated but rather is expressed at higher levels, in inappropriate cells or at inappropriate times. Rab GTPases play a master role in regulating intercellular vesicle trafficking in both exocytic and endocytic pathways. (Stein *et al.*, 2003). Studies have demonstrated links between Rab GTPase dysfunction in human diseases such as Griscelli syndrome type 2 and thyroid-associated adenomas, which are caused by mutation of the *RAB27a* gene (Menasche *et al.*, 2000) and up-regulation of *RAB5a* and *RAB7* (Croizet-Berger *et al.*, 2002), respectively. In addition, dysregulation of *RAB* gene expression, in particular *RAB25*, may be a generalized component regulating the aggressiveness and potentially the outcome of human cancers, as increased *RAB25* levels have been noticed in cancers including ovarian and breast cancers (Cheng *et al.*, 2004), prostate cancer (Calvo *et al.*, 2002), transitional cell carcinoma of the bladder (Mor *et al.*, 2003), and invasive breast tumor cells (Wang *et al.*, 2002), suggesting a pathological role of Rab25 proteins in the development or progression of tumors in multiple epithelial lineages. However, the molecular mechanism by which Rab25 mediates its functions remains unknown. Here, we describe a molecular approach to examine the functional role of Rab25 in cancers.

We have instituted a generalized approach that can be broadly applied to identify drivers of genomic aberrations. In the process, areas of genomic aberrations are mapped as finely as possible using array comparative genomic hybridization (CGH) (Hodgson *et al.*, 2001; Pinkel *et al.*, 1998).

If there are many candidate regions, we select those that correlate with the patient's outcome, as these are more likely to harbor targets for therapy. To identify genes that are dysregulated by genomic amplification, we identify all of the open reading frames in the region using the University of Santa Cruz genome browser (<http://genome.cse.ucsc.edu/>) and utilize publicly available transcriptional profiling (Oncomine cancer microarray database) and SAGE (<http://cgap.nci.nih.gov/>) databases to determine levels of increases in transcripts in the tumor of interest. Any transcripts in which data are not available as well as candidates from the transcriptional profiling and SAGE analysis are assessed by quantitative polymerase chain reaction (PCR). We put a major emphasis on coordinate amplification at the CGH and RNA level and correlation with outcomes, which can provide a filter to identify genes, which are more likely to be therapeutic targets. Once candidate genes are identified, we perform functional genomics by manipulating levels in normal and tumor cells using RNAi (Milhavet *et al.*, 2003) or transfection with expression constructs, and assessing a battery of cellular functions including proliferation, anti-apoptosis, loss of contact inhibition, changes in cell signaling or transcriptional profiles, anchorage-independent growth, and *in vivo* tumor growth (Fig. 1).

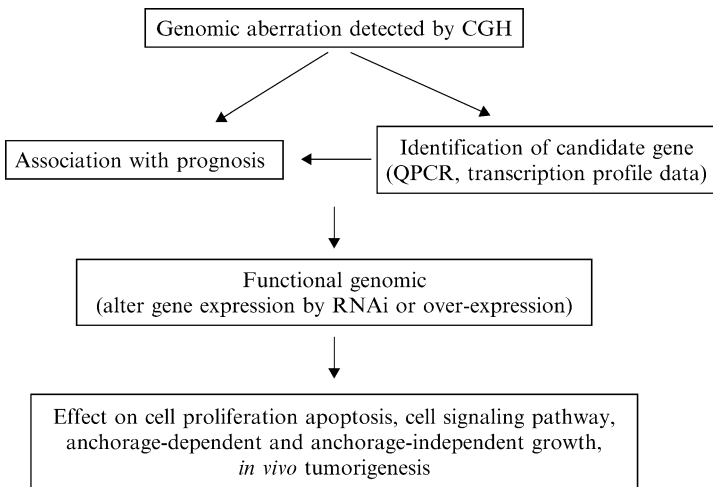


FIG. 1. Diagrammatic representation of the approach in identifying drivers of genomic aberration and its functional role. Emphasis was placed on coordinate amplification at the CGH and RNA level and correlation with outcomes, which provide a filter to identify potential therapeutic target gene(s).

### Isolation and Quantitative Real-Time Polymerase Chain Reaction (QPCR)

To determine levels for the *RAB25*, total RNA was isolated from 10 ovarian and breast cancer cell lines using Trizol reagent (Invitrogen, Carlsbad, CA) according to the manufacturer's suggested protocol. QPCR was analyzed with an ABI PRISM 7700 Sequence Detection system from Applied Biosystems (Foster City, CA) with a *RAB25*-specific mix of unlabeled PCR primer and Taqman MGB probe (20× concentrations) using TaqMan One-Step RT-PCR Master Mix Reagent Kit (Applied Biosystems, Foster City, CA). The sequences of the *RAB25* forward and reverse PCR primers are 5'-CTGAGGAGGCCCGAATGTT-3' and 5'-GGCTGAGGTCTCCAGGAAGAG-3', respectively, and the Taqman MGB probes sequence is 5'-CGCTGAAACAATGGA-3'. The MGB probe was labeled at the 5' end by a fluorescent FAM dye and quenched by TAMRA dye at the 3' end. The forward and reverse primers are located at exons 3 and 4, respectively, whereas the *RAB25* probe resides at the boundary of exon 3 and exon 4. With this probe, one messenger RNA will be detected. QPCR was performed by mixing 60 ng of total RNA with 25  $\mu$ l of 2× Master mix without UNG, 1.25  $\mu$ l of 40× MultiScribe and RNase Inhibitor Mix, and 2.5  $\mu$ l of the 20× primer and probe to a final volume of 50  $\mu$ l. The reverse transcription was carried out by incubating the mixture at 48° for 30 min, heating at 95° for 10 min, followed by 40 PCR cycles at 95° for 15 s and 60° for 60 s. To normalize the amount of total RNA present in each reaction,  $\beta$ -actin genes were used as an internal standard.

### Preparation of *RAB25* Expression Constructs

Total RNA isolated from ovarian cancer OVCAR3 cells was used as a template for PCR amplification to generate a 652-base pair human *RAB25* full-length cDNA using *RAB25*-specific sense (5'-CGAAGCTTATG-TACCCATACGATGTTCCAGATTACGCTGGGAATGGAAGAT-3') and antisense (5'-GTGGATCCGAGGGGTGGACAGATAAAAGAGGTATT-3') primers. *Hind*III (AAGCTT) and *Bam*HI (GGATCC) recognition sites (underlined) were introduced to facilitate the cloning procedure, and a hemagglutinin (HA)-tagged sequence (TACCCATACGATGTTCCAGATTACGCT) was fused with the *RAB25* sequence after the ATG start codon to help in identifying the recombinant Rab25 protein. cDNA was synthesized from total RNA using the First Strand cDNA synthesis kit following the manufacturer's instructions (Invitrogen, Carlsbad, CA). The reaction mixture (15  $\mu$ l), containing 5  $\mu$ g total RNA, 5  $\mu$ l bulk first-strand reaction mix, 0.2  $\mu$ g oligo(dT) primer,

and 6 mM dithiothreitol (DTT), was incubated at 37° for 60 min and terminated by heating at 90° for 5 min. To amplify the *RAB25* cDNA, 5  $\mu$ l reverse-transcribed cDNA was subjected to PCR amplification in a 50- $\mu$ l reaction mix containing 10 mM Tris-HCl, pH 8.3, 50 mM KCl, 2.5 mM MgCl<sub>2</sub>, 0.001% w/v gelatin, 10 mM each of dATP, dCTP, dTTP, and dGTP, 2.5 units of *Taq* polymerase (Invitrogen, Carlsbad, CA), and 20 pmol of each sense and antisense primer with the conditions of denaturation at 94° for 60 s, primer annealing at 55° for 65 s, and extension at 72° for 90 s. The PCR product was digested with *Hind*III and *Bam*HI, and ligated into pcDNA3.1 (+) vector to generate the HA-tagged Rab25 expression construct (Invitrogen, Carlsbad, CA). The insert was sequenced to confirm the presence of the correct open reading frame.

### Transfection and Clonal Selection

Human epithelial ovarian carcinoma A2780, DOV13, HEY, and OCC1 cell lines were cultured in RPMI 1640 supplemented with 10% fetal bovine serum (FBS) (Atlanta Biologicals, Norcross, GA). All of the cell lines were tested to evaluate G418 (Invitrogen, Carlsbad, CA) resistance. G418 was applied in a concentration from 200 to 1000  $\mu$ g/ml. The lowest concentration of G418 that killed all of the cells was applied later in the clonal selection. Stable *RAB25* expressing clones were generated by transfecting ovarian cells ( $1 \times 10^5$ ) seeded into 60-mm tissue culture plates 1 day before transfection. Two micrograms of the HA-tagged Rab25 expression construct was mixed with 6  $\mu$ l of Fugene 6 reagent (Roche Molecular Biochemicals) in 100  $\mu$ l of serum-free medium. The DNA mixture was incubated for 20 min at room temperature and then applied to the cells. Incubation of the cells with transfection medium was continued for approximately 24 h at 37° in 5% CO<sub>2</sub>. After transfection, the cells were washed twice with culture medium and incubated with normal culture medium containing 10% FBS. *RAB25* stably-expression clones were selected for 4–6 weeks by limiting dilution in the presence of G418.

Positive clones were identified by Western blotting analysis. Cells were lysed in ice-cold lysis buffer (1% Triton X-100, 50 mM HEPES, pH 7.4, 150 mM NaCl, 1.5 mM MgCl<sub>2</sub>, 1 mM EGTA, 100 mM NaF, 10 mM Na-pyrophosphate, 1 mM Na<sub>3</sub>VO<sub>4</sub>, 10% glycerol, 1 mM phenylmethylsulfonyl fluoride [PMSF], and 10 g/ml aprotinin) for 15 min on ice. After lysis, the samples were centrifuged at 14,000 rpm for 10 min at 4°, and the supernatants were stored at –80°. Proteins were diluted in sample loading buffer (5 $\times$ : 60 mM Tris-HCl, pH 6.8, 25% glycerol, 2% sodium dodecyl sulfate (SDS), 14.4 mM 2-mercaptoethanol, 0.1% bromophenol blue), boiled for 5 min, separated by SDS-polyacrylamide gel electrophoresis (PAGE), and transferred to

Hybond-ECL nitrocellulose membranes (Amersham Bioscience). Blots were blocked with TBST (25 mM Tris-HCl, pH 7.5, 150 mM NaCl, 0.1% Tween-20) containing 5% bovine serum albumin for at least 1 h and probed with monoclonal antibody HA.11 (1:1000 dilution; Covance, Berkeley, CA) against HA epitope overnight. The membrane was washed six times in TBST, 5 min each, and incubated with secondary antibodies coupled to horseradish peroxidase (HRP) for 1 h at room temperature. The signal was visualized by an enhanced chemiluminescence detection ECL system (Amersham Bioscience) after extensive washing in TBST.

### Colony Formation Assay

For anchorage-dependent colony formation,  $1 \times 10^4$  cells were transfected with either pCDNA 3.1 or *RAB25* expression vector. Forty-eight hours posttransfection, cells were trypsinized and replated in two six-wells/plate for 14 days in the presence of G418. Cells were stained with 0.1% Coomassie blue (Bio-Rad) in 30% methanol and 10% acetic acid. The number of colonies formed was counted and expressed as fold increase compared with pCDNA transfected cells.

To test the effect of *RAB25* expression on anchorage-independent colony formation, pCDNA or *RAB25* stable expressing cells were suspended at a density of  $1 \times 10^4$  cells/ml in 1.5 ml of 0.3% agar (Bacto-agar; Difco, Detroit, MI) dissolved in complete medium containing 25% FBS (top layer). Cells were plated in 35-mm dishes precoated with 1.5 ml of solidified 0.6% agar base in complete medium containing 25% FBS (bottom layer). After 3 days of incubation, 200  $\mu$ l fresh complete medium supplemented with 5% FBS was added to maintain humidity. Colony-forming efficiency was measured 14–18 days after plating (greater than 50 cells/colony) under a microscope and expressed as a fold increase related to control vector transfected cells.

### Apoptosis Assays

Apoptosis was induced by culturing cells in 0.1% serum for 48 h, by UV radiation or by paclitaxel. The intensity of UV radiation ( $\mu$ J/cm<sup>3</sup>) and the concentrations of paclitaxel (ng/ml) required to induce apoptosis were predetermined by exposing the untransfected cells to various intensities of UV radiation (50–400  $\mu$ J/cm<sup>3</sup>) and concentrations of paclitaxel (50–200 ng/ml). Cells were then harvested and assayed for apoptosis by flow cytometry as described below after 24 and 48 h. The lowest intensity of UV radiation and concentration of paclitaxel that induce approximately 50% of cells to undergo apoptosis were applied later to examine the effect of

*RAB25* overexpression or down-regulation on cell death. For anoikis assays, cells were incubated on a rocker platform to prevent adhesion for 48 h. In each experiment, both floating and attached cells ( $1-2 \times 10^6$  cells) were collected after treatment and washed twice with phosphate-buffered saline (PBS; 10 mM sodium phosphate, pH 7.2, 150 mM sodium chloride). Cells were then fixed with 1% (w/v) paraformaldehyde in PBS for 15 min on ice. Cells were collected by centrifugation at  $300\times g$  for 5 min and washed twice with PBS. After washing, cells were resuspended in 5 ml ice-cold 70% ethanol and stored in ice for at least 30 min before measuring apoptotic cells using an APO-BrdU kit (Phoenix Flow Systems, Inc., San Diego, CA) with a FACScan (Beckton Dickinson) cell sorter, air-cooled argon laser 488 nm, using CellQuest software. pcDNA transfected cells were included as control.

#### *In Vivo* Tumorigenicity Assay

To assess the impact of *RAB25* overexpression on tumorigenicity, five female BALB/c *nu/nu* mice (4 weeks old) were inoculated with either *RAB25*-overexpressing or pcDNA-transfected control cells. Animals were housed in a sterile, air-conditioned atmosphere, given food and water in standard conditions, and handled in a sterile laminar flow hood. Subcutaneous and intraperitoneal injections were performed with  $5 \times 10^6$  cells in 0.2 ml PBS. Tumor development was monitored once a week. Subcutaneous tumors were measured with a digital caliper. The length (*L*) and width (*W*) of each tumor were measured to calculate tumor volume (*V*) as follows:  $V = 2W(L/2)^2$ . Intraperitoneal tumor mass was measured by dissection of the tumor from the peritoneal cavity and weighing.

#### RNA Interference

Chemically synthesized *RAB25*-specific siRNA (5'-GGAGCUCUAU-GACCAUGCU-3') was purchased from Xeragon, now part of Qiagen (Valencia, CA). A scramble RNAi negative control was purchased from Ambion. RNAi transfection was carried out in solution T using a Nucleofector system (Amaxa Biosystem). At the day of transfection,  $1 \times 10^6$  *RAB25* stably expressed A2780 or breast MCF-7 cells were harvested and resuspended in 100  $\mu$ l of solution T. Then 5  $\mu$ l of *RAB25* SiRNA (20  $\mu$ M) was added to the cell suspension and the mixture was transferred into an electroporation cuvette (Amaxa Biosystem). The cuvette was inserted into a Nucleofector system and transfection was carried out using Nucleofector program R23. Immediately after transfection, 500  $\mu$ l of complete medium was added to the cells and transferred into six-well plates.

### Reverse-Phase Protein Lysate Array (RPPA)

*RAB25*-overexpressing or pcDNA-transfected control A2780 cells ( $5 \times 10^5$ ) were serum starved for 24 h before stimulation with IGF, EGF, TGF- $\beta$ , and FBS for 5 min, 30 min, 2 h, and 24 h. Total cellular protein were isolated by lysis buffer as previously described. Protein concentration was determined by BCA reaction (Pierce Biotechnology, Inc., Rockford, IL) and adjusted to 1  $\mu\text{g}/\mu\text{l}$  by diluting in 4 $\times$  sodium dodecyl sulfate (SDS) buffer (250 mM Tris-HCl, pH 6.8, 35% glycerol, 8% SDS, 10% 2-mercaptoethanol) to a final 1 $\times$  concentration. The samples were then boiled for 5 min and a serial 2-fold dilution was prepared using diluted lysis buffer in 4 $\times$  SDS buffer. To each diluted sample, an equal amount of 80% glycerol/2 $\times$  PBS solution (8 ml glycerol mixed with 2 ml of 10 $\times$  PBS without  $\text{Ca}^{2+}$  and  $\text{Mg}^{2+}$ ) was added. The samples were ready for printing.

Protein lysate arrays were printed on nitrocellulose-coated glass slides (FAST Slides, Schleicher & Schuell) by a GeneTAC G3 arrayer (Genomic Solution, Ann Arbor, MI) with Forty 75- $\mu\text{m}$ -diameter pins arranged in a 4  $\times$  10 format. Forty grids were printed at each slide with each grid contained 16 dots. Protein dots were printed in duplicate with eight concentrations (from undiluted to 1/128-fold diluted samples). Arrays were produced in batches of 10, and the occasional low-quality array (e.g., with many spot dropouts) was discarded.

Each array was incubated with a specific primary antibody and the signal was detected by using the catalyzed signal amplification (CSA) system according to the manufacturer's recommended procedure (DakoCytomation California, Inc., Carpinteria, CA). In brief, each slide was blocked with I-block (Applied Biosystems, Foster City, CA) overnight at 4 $^\circ$ . After blocking, the slide was incubated with primary antibody and secondary antibody, diluted in DAKO antibody diluent with background reducing compound, at room temperature for 1 h and 45 min, respectively. The slide was then incubated with streptavidin-biotin complex, biotinyl tyramide (for amplification) for 15 min, streptavidin-peroxidase for 15 min, and 3,3'-diaminobenzidine tetrahydrochloride chromogen for 5 min. Between steps, the slide was washed with TBST. The signal was scanned with an HP Scanjet 8200 scanner (Hewlett Packard, Palo Alto, CA) with a 256-shade gray scale at 600 dots per inch. Spot images were converted to raw pixel values by Microvigene version 2.0 (VigeneTech, North Billerica, MA).

### Comment

In our studies, Rab25 was initially implicated in ovarian cancer by being located at a site of genomic amplification in ovarian cancer. Genomic amplification is indicative of selection for a gene or genes in the region.

Using QPCR, we measured the endogenous expression level of *RAB25* in 10 ovarian and breast cancer cell lines (Fig. 2). Normal ovarian surface epithelium was used to set the baseline for comparison. With RNA, identification of the appropriate control is a major challenge. In many cases, the cell of origin for a tumor is not known or cannot be prepared in large quantities. Further, if cancer arises in a limited population of stem cells in the precursor lineage, it may be difficult to purify sufficient cells for comparison. Identification of cancer cells with high and low endogenous *RAB25* levels provided a powerful tool in studying the functional role of *RAB25* in cancer. Altering *RAB25* levels in cell lines with *RAB25* expression constructs resulted in increasing anchorage-independent colony-forming activity (Fig. 3), cell proliferation, and cell survival under multiple stress conditions including serum starvation, anoikis (anchorage-independent stress), UV radiation and chemotherapy (paclitaxel), and *in vivo* tumor formation in murine xenografts as recently reported

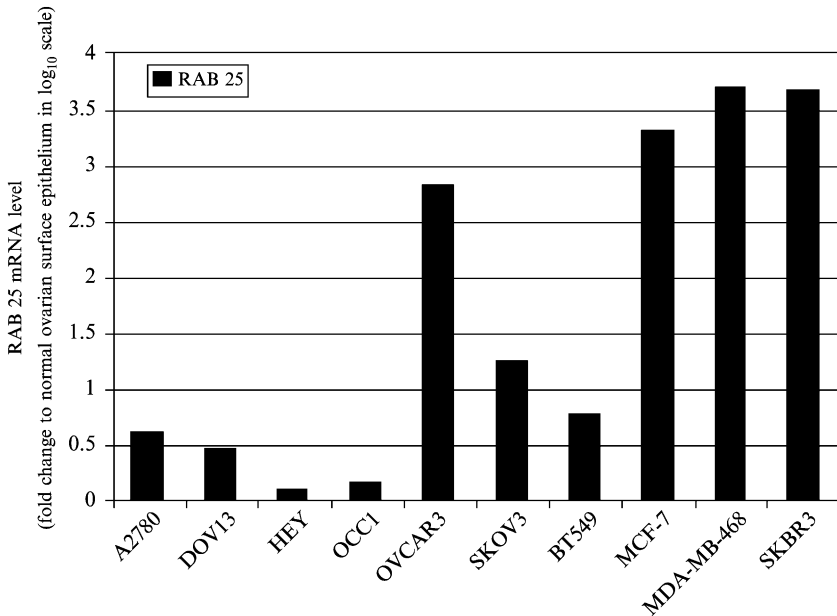


FIG. 2. Quantification of *RAB25* mRNA level in human ovarian and breast cancer cells by real-time quantitative polymerase chain reaction. Total RNA was isolated from ovarian cancer A2780, DOV13, HEY, OCC1, OVCAR3, and SKOV3, and breast cancer BT549, MCF-7, MDA-MB-468, and SKBr3 cells. The *RAB25* mRNA level in normal ovarian surface epithelium was included and set as baseline for comparison.

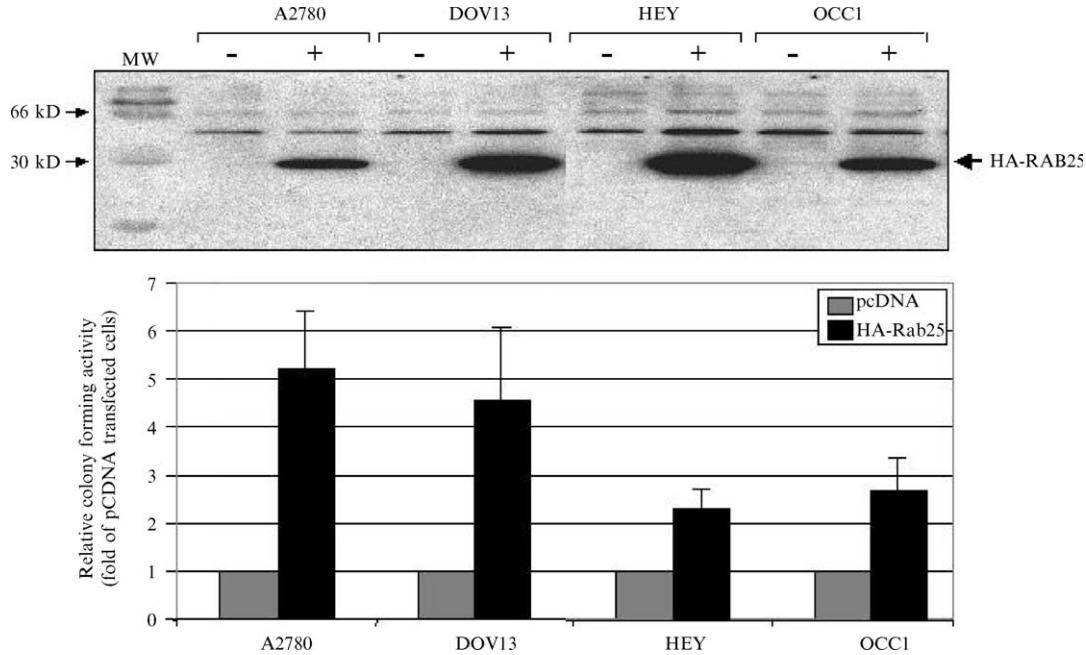


Fig. 3. *RAB25* regulates cell survival. Western blot analysis of HA-tagged RAB25 expression in ovarian cancer A2780, DOV13, HEY, and OCC1 cells (upper panel). The expression of RAB25 increases the colony-forming ability of ovarian cancer cells. Ovarian cancer cells were transfected with HA-tagged RAB25 expression construct or pCDNA control construct. The total number of colonies was counted 14 days after selection in medium containing G418, and shown as folds increase compared with pCDNA transfected cells. Results are the mean  $\pm$  SD from three individual experiments.

(Cheng *et al.*, 2004). In addition, decreasing the expression of *RAB25* by RNAi transfection significantly decreased cell proliferation and markedly increased the sensitivity to apoptosis of both breast and ovarian cancer cells, confirming the role of *RAB25* in mediating cell survival (Cheng *et al.*, 2004).

A recent study has provided direct evidence that multiple signaling molecules including AKT, ERK1/2, and p38MAPK associate on endocytic vesicles and mediate their function by translocation of the vesicle to the nucleus, providing a potential mechanism by which Rab GTPases conduct cell survival signals (Delcroix *et al.*, 2003). We were able to demonstrate an increase in AKT phosphorylation in *RAB25*-overexpressed A2780 cells by Western blotting analysis (Cheng *et al.*, 2004). However, this approach is time and labor intensive. As a result, a high-throughput lysate array technology (RPPA) was introduced to dissect potential Rab25-mediated signal transduction pathways. In our hands, at least 160 samples can be examined simultaneously in one slide (Fig. 4A has 40 examples). Our data confirmed the increase in AKT phosphorylation in *RAB25*-overexpressed

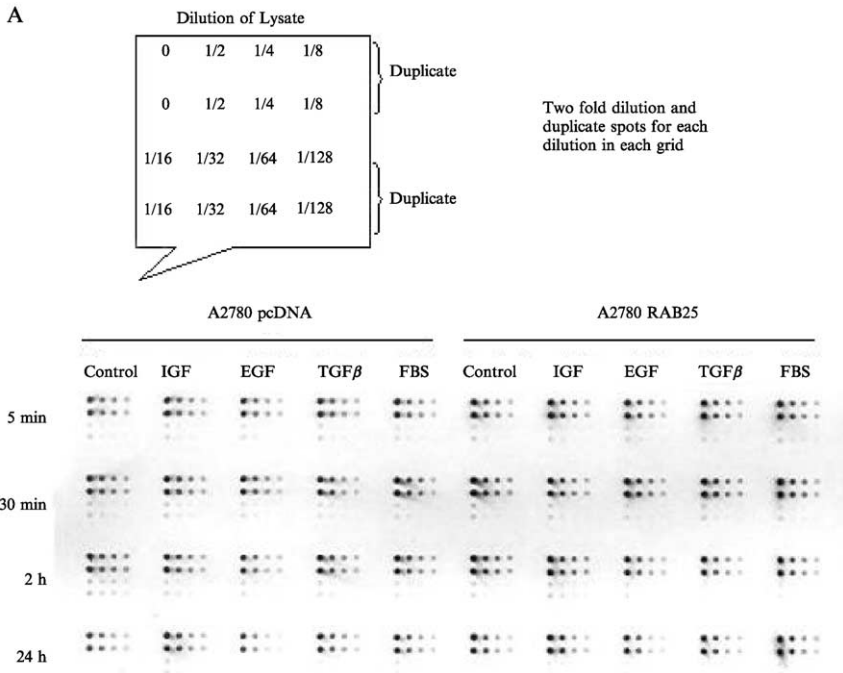


FIG. 4. (continued)

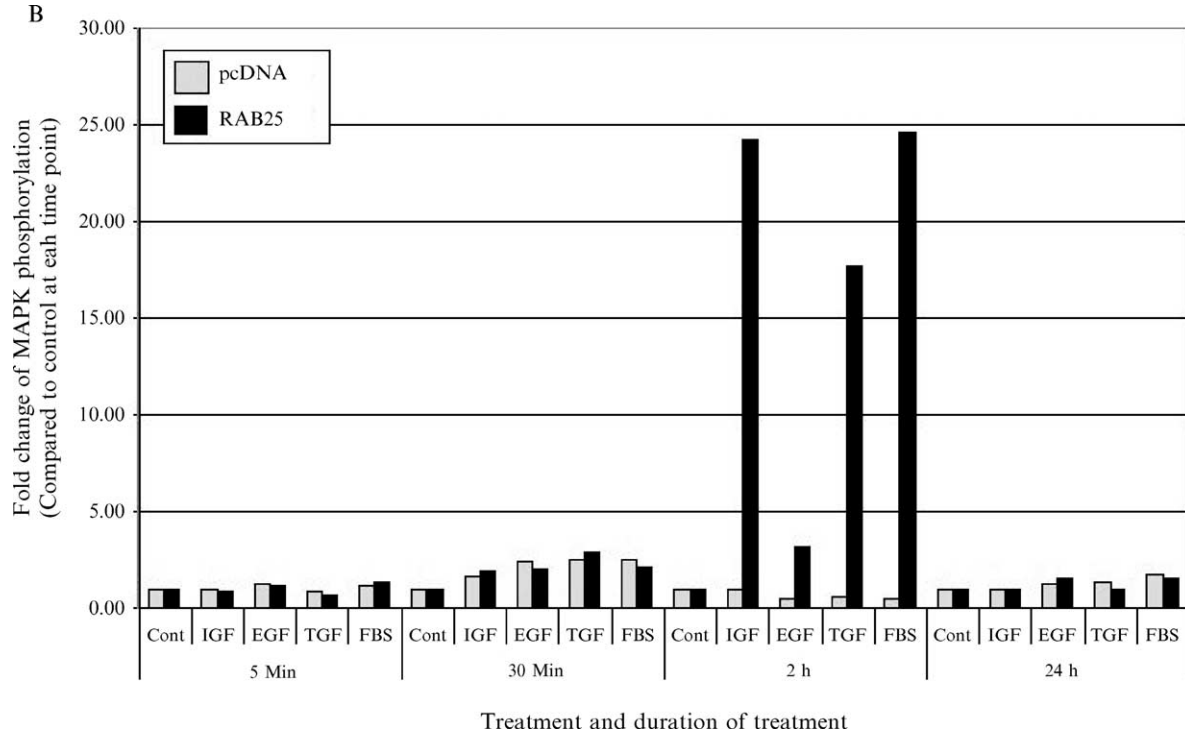


FIG. 4. Protein lysate array analysis. (A) Total cellular proteins was isolated from *RAB25* stable expressed ovarian cancer A2780 cells after treating with insulin growth factor (IGF), epithelial growth factor (EGF), transforming growth factor- $\beta$  (TGF $\beta$ ), and fetal bovine serum (FBS) for 5 min, 30 min, 2 h, and 24 h. Protein dots were printed in duplicate with eight concentrations (from undiluted to 1/128-fold diluted samples). A typical protein array slide was shown. (B) Effect of *RAB25* expression on MAPK phosphorylation. The change in MAPK phosphorylation was normalized with the total MAPK level and compared to the control sample at each time point.

TABLE I  
ANTIBODIES USED IN PROTEIN LYSATE ARRAY STUDY

Antibody	Source	Cat. #	Dilution
Total AKT	Cell Signaling	9272	250
AKT (phospho-Ser 473)	Cell Signaling	9271	250
AKT (phospho-Thr 308)	Cell Signaling	9275	250
c-Abl	Cell Signaling	2862	500
c-Cbl	BD Transduction Lab	610441	500
EGFR	Sigma	E3138	1000
EGFR (Phospho-Tyr 992)	Cell Signaling	2234	100
EGFR (Phospho-Tyr 1068)	Cell Signaling	2235	100
JNK	Santa Cruz	SC-474	1000
JNK (Phospho-Thr 183/Tyr 185)	Cell Signaling	9251	200
Total MAPK	Cell Signaling		
MAPK (Phospho-p40/42)	Cell Signaling	9101	1000
mTOR	Cell Signaling	2972	250
mTOR (Phospho-Ser 2448)	Cell Signaling	2971	250
GAPDH	Ambion	4300	10000

cells. In addition, using robotic replication of slides and staining with multiple validated antibodies, we are able to examine the effect of Rab25 on multiple signal transduction molecules (Table I). For example, an increase in MAPK phosphorylation was observed in *RAB25*-overexpressed A2780 cells after 2 h of stimulation but not in 5 min, 30 min, and 24 h stimulation when compared to corresponding controls at each time point (Fig. 4B). These results have high reproducibility as similar signals and trends are obtained from total cellular lysate isolated from reproduced experiments. Profiling multiple signal transduction molecules by lysate array technology will certainly facilitate our understanding of the molecular mechanism by which *RAB25* regulates the aggressiveness of cancers.

### Acknowledgments

K.W.C. was supported by the Odyssey Program of the Houston Endowment Scientific Achievement award from the MD Anderson Cancer Center. This work is supported by National Institutes of Health SPORE (P50-CA83639) and PPG-PO1 CA64602 to G.B.M.

### References

Calvo, A., Xiao, N., Kang, J., Best, C. J., Leiva, I., Emmert-Buck, M. R., Jorcyk, C., and Green, J. E. (2002). Alterations in gene expression profiles during prostate cancer

- progression: Functional correlations to tumorigenicity and down-regulation of seleno-protein-P in mouse and human tumors. *Cancer Res.* **62**, 5325–5335.
- Cavaneae, W. K., and White, R. L. (1999). The genetic basis of cancer. *Sci. Am.* **275**, 72–79.
- Cheng, K. W., Lahad, J. P., Kuo, W. L., Lapuk, A., Yamada, K., Auersperg, N., Liu, J., Smith-McCune, K., Lu, K. H., Fishman, D., Gray, J. W., and Mills, G. B. (2004). The RAB25 small GTPase determines aggressiveness of ovarian and breast cancers. *Nat. Med.* **10**(11), 1251–1256.
- Croizet-Berger, K., Daumerie, C., Couvreur, M., Courtoy, P. J., and van den Hove, M. F. (2002). The endocytic catalysts, Rab5a and Rab7, are tandem regulators of thyroid hormone production. *Proc. Natl. Acad. Sci. USA* **99**(12), 8277–8282.
- Delcroix, J. D., Valletta, J. S., Wu, C., Hunt, S. J., Kowal, A. S., and Mobley, W. C. (2003). NGF signaling in sensory neurons: Evidence that early endosomes carry NGF retrograde signals. *Neuron* **39**, 69–84.
- Hanahan, D., and Weinberg, R. A. (2000). The hallmark of cancer. *Cell* **100**, 57–70.
- Hodgson, G., Hager, J. H., Volik, S., Hariono, S., Wernick, M., Moore, D., Nowak, N., Albertson, D. G., Pinkel, D., Collins, C., Hanahan, D., and Gray, J. W. (2001). Genome scanning with array CGH delineates regional alterations in mouse islet carcinomas. *Nat. Genet.* **29**(4), 459–464.
- Menasche, G., Pastural, E., Feldmann, J., Certain, S., Ersoy, F., Dupuis, S., Wulffraat, N., Bianchi, D., Fischer, A., Le Deist, F., and de Saint Basile, G. (2000). Mutations in RAB27A cause Griscelli syndrome associated with haemophagocytic syndrome. *Nat. Genet.* **25**(2), 173–176.
- Milhavet, O., Gary, D. S., and Mattson, M. P. (2003). RNA interference in biology and medicine. *Pharmacol. Rev.* **55**, 629–648.
- Mor, O., Nativ, O., Stein, A., Novak, L., Lehavi, D., Shibolet, Y., Rozen, A., Berent, E., Brodsky, L., Feinstein, E., Rahav, A., Morag, K., Rothenstein, D., Persi, N., Mor, Y., Skaliter, R., and Regev, A. (2003). Molecular analysis of transitional cell carcinoma using cDNA microarray. *Oncogene* **22**, 7702–7710.
- Pinkel, D., Segraves, R., Sudar, D., Clark, S., Poole, I., Kowbel, D., Collins, C., Kuo, W. L., Chen, C., Zhai, Y., Dairkee, S. H., Ljung, B. M., Gray, J. W., and Albertson, D. G. (1998). High resolution analysis of DNA copy number variation using comparative genomic hybridization to microarrays. *Nat. Genet.* **20**(2), 207–211.
- Stein, M. P., Dong, J., and Wandinger-Ness, A. (2003). Rab proteins and endocytic trafficking: Potential targets for therapeutic intervention. *Adv. Drug Deliv. Rev.* **55**(11), 1421–1437.
- Wang, W., Wyckoff, J. B., Frohlich, V. C., Oleynikov, Y., Huttelmaier, S., Zavadil, J., Cermak, L., Bottinger, E. P., Singer, R. H., White, J. G., Segall, J. E., and Condeelis, J. S. (2002). Single cell behavior in metastatic primary mammary tumors correlated with gene expression patterns revealed by molecular profiling. *Cancer Res.* **62**, 6278–6288.
- Weinberg, R. A. (1996). How cancer arises. *Sci. Am.* **272**, 62–70.